Exciton and trion formation in systems with van Hove singularities

Lewis J. Burke,* Mark T. Greenaway,† and Joseph J. Betouras‡
Department of Physics and Centre for the Science of Materials,
Loughborough University, Loughborough LE11 3TU, United Kingdom
(Dated: November 21, 2025)

We investigate the role of van-Hove singularities (VHS) in a system's electronic band structure, on the formation and properties of excitons and trions. We consider (i) the different parameters of a Mexican-hat-type dispersion of the valence band, which hosts a VHS at the band edge, and (ii) the presence of regular VHS or higher-order VHS (HOVHS). We find that for a given spin-degenerate Mexican-hat-shaped valence band, where a trion and exciton can form, trion formation becomes more favourable as the Mexican-hat dispersion becomes narrower. Also, we show that if the electronic band structure contains an HOVHS, then both the exciton and trion dispersion will also contain such a singularity. Therefore, a HOVHS in the valence band can suitably change the density of states (DOS) of the bound-state particle and lead to the generation of new states, which could impact the optical properties of the system. Our work provides a pathway to how 2D quantum materials, which host such singularities, can be engineered to favour a particular bound-state thus opening new avenues for these materials into potential applications.

I. INTRODUCTION

Excitons are neutrally charged quasiparticles comprised of electrostatically bound electron-hole pairs generated under an optical excitation of the material via absorption of a photon [1]. They play a crucial role in the electronic and optical properties of quantum materials. Excitons are typically studied in intrinsic semiconductor systems. However, electron or hole doping allows the formation of a bound three-particle complex comprised of the initial exciton electron-hole pair bound to the free charge carrier, known as a trion or charged exciton [2]. These systems have been studied in a variety of materials from transition metal dichalcogenides (TMDs) [3-8], to other hexagonal chalcogenides such as InSe [9, 10]. These bound states are not limited to monolayer systems and can also form in bilayer (and multilayer) systems, in which interlayer excitons and Moiré excitons and trions can form [11, 12].

Understanding these bound states is crucial for determining how light interacts with these quantum materials. Trions are of particular interest because of their charged nature. Previous work has shown the ability to control such trions via an electric field [13], meaning that they can move like a free charge carrier. However, unlike an electron, a trion has additional degrees of freedom encoded in its state. To understand how to exploit this property for applications such as the transport of information, we need more insight into the properties of these quasiparticles [14]. In order that these quasi-particles can be used in a wide set of applications, they should remain in a bound state for a significant length of time. One way to extend the lifetime of these states is to create "dark" quasi-particle states, where recombination occurs via to

a multi-step process, in contrast to bright states which recombine directly [15–18].

In this work, we study the formation and strength of the binding energy of these quasi-particle states in 2D monolayer systems. In particular, we consider systems in which the valence band exhibits a Mexican-hat shaped dispersion and the conduction band is parabolic with a constant effective mass. Van-Hove singularities occur when the gradient of the energy dispersion, denoted by $\nabla_k E(\mathbf{k})$, vanishes [19]. This leads to a divergent density of states (DOS) of the quasiparticle. In addition, when the Hessian of the energy dispersion also vanishes the system exhibits a higher-order van Hove singularity (HOVHS) with a power-law divergence of the DOS [20]. This is in contrast to the logarithmic divergence in a 2D system, which occurs at the VHS when the Hessian is nonzero.

Recently, work on systems with HOVHSs has shown how they provide an important role in phase formation. thermodynamics and the transport properties of the materials [21–23]. However, their effects on the properties of exciton and trions are not well understood. In a previous work, [10], we showed that the underlying band structures of the trion system strongly influences the binding energy of the quasiparticles. It was found that for monolayer InSe, the negative trion (comprising two electrons in the parabolic conduction band) leads to a bound trion state, whilst the positive trion is unbound (comprising holes at the VHS of the Mexican-hat valence band). In this case, the VHS in the valence band determined the binding of the quasi particle such that the unbound nature was found to be due to the enhanced hole-hole interaction at the VHS.

Here, we focus on the effect of varying the form of the top-most valence band on the properties of the exciton and positive trion states. In particular, we examine how sensitive the bound states are to the different aspects of the Mexican-hat system as exhibited by many hexagonal chalcogenides [9, 24] or multilayer systems. We will con-

^{*} L.J.Burke@lboro.ac.uk

[†] M.T.Greenaway@lboro.ac.uk

[‡] J.Betouras@lboro.ac.uk

sider the influence of the width and depth of the Mexicanhat, the conduction band effective mass, the dielectric environment of the system, and the effect of HOVHS.

In real systems, it has been shown the Mexican-hat shape of a different width and depth, and the electron effective masses, lead to differences in the binding energy of the bound states. In Ref [9], InSe with different thickness was studied, and it was shown that for monolayer to bilayer, the exciton energy of the ground state (taken as the 0s state) is reduced. This can be understood in part due to the change in conduction and valence band energies. However, the interaction effects also change when one moves to a bilayer. This is due to the screening length becoming twice that of the monolayer system, which impacts the bound state. Therefore, to disentangle these effects we focus on the effect of the bound states due to the change of the electronic band structure and how this impacts the ground-state exciton. The choice of the positive trion in this work stems from a general investigation of a system in which the like charges in the trion are both governed by a Mexican-hat shaped dispersion. Thus, the same results from this paper would be true for the negative trion in this setup. Our previous work on monolayer InSe highlighted how unfavourable this system is in comparison to the excitonic system, thus, investigating the cause of this is important for future potential applications.

The structure of the paper is that in Section. II we present the model and the fundamental equations to be solved; in Section III, there is a detailed analysis related to the parameters of the Mexican-hat dispersion; section IV is devoted to HOVHS; and we conclude and discuss the findings in Section V. Details of the calculations are provided in the Appendices.

II. MODEL AND METHOD

We employ the variational technique to find the quasiparticle dispersion. We minimise the expectation value of the exciton and trion energies to obtain an upper bound on the binding energy of their ground states [10]. For the exciton, the energy eigenvalue equation is:

$$E_{ex}\phi_{ex}(\mathbf{k}) = [E_c(\mathbf{k}) - E_v(\mathbf{k} - \mathbf{Q})]\phi_{ex}(\mathbf{k}) + \frac{1}{A} \sum_{\mathbf{q}} \phi_{ex}(\mathbf{k} - \mathbf{q})V(\mathbf{q})$$
(1)

where $E_{c/v}(\mathbf{k})$ are the conduction/valence band energies and $V(\mathbf{q})$ is the Rytova-Keldsh Coulomb interaction [25, 26]:

$$V(\boldsymbol{q}) = \frac{-2\pi e^2}{\sqrt{\kappa_z \kappa_{||}}} \frac{1}{|\boldsymbol{q}|(1 + r_0|\boldsymbol{q}|)},$$
 (2)

where r_0 is the screening length:

$$r_0 = \frac{\sqrt{\varepsilon_z \varepsilon_{||}} - 1}{2\sqrt{\kappa_z \kappa_{||}}} d, \tag{3}$$

and $\varepsilon_z, \varepsilon_{||}$ are the in and out-of-plane permittivity of the 2D material and $\kappa_z, \kappa_{||}$ are the permittivities of the dielectric environment that encompasses it. Here, we use the values of monolayer InSe described in Ref. [9]. The sums over the Brillouin zone were done using the Monkhorst-Pack grid [27, 28]. In Appendix. A we show the effect of varying the permittivities of the material on the exciton binding energy. We assume a hydrogenic states for the exciton variational wavefunction so that for the ground state exciton we use the 1s hydrogenic wave function, which in momentum space is:

$$\phi_{ex}(\mathbf{k}) = \frac{1}{(\beta^2 + k_x^2 + k_y^2/\lambda^2)^{3/2}}$$
(4)

where β , λ are the unknown variational parameters. β is the inverse exciton radius and λ is an anisotropy parameter. The corresponding expression for the energy of the positive trion, $E_{tr,+}(\mathbf{Q})$, is [10]:

$$E_{tr,+}(\boldsymbol{Q})\phi_{tr}(\boldsymbol{k}_{1},\boldsymbol{k}_{2}) =$$

$$\left[E_{c}(\boldsymbol{k}_{1}+\boldsymbol{k}_{2})-E_{v_{1}}(\boldsymbol{k}_{1}-\boldsymbol{Q})-E_{v_{2}}(\boldsymbol{k}_{2})\right]\phi_{tr}(\boldsymbol{k}_{1},\boldsymbol{k}_{2})$$

$$+\sum_{\boldsymbol{q}}V(\boldsymbol{q})\phi_{tr}(\boldsymbol{k}_{1}-\boldsymbol{q},\boldsymbol{k}_{2})+\sum_{\boldsymbol{q}}V(\boldsymbol{q})\phi_{tr}(\boldsymbol{k}_{1},\boldsymbol{k}_{2}-\boldsymbol{q})$$

$$-\sum_{\boldsymbol{q}}V(\boldsymbol{q})\phi_{tr}(\boldsymbol{k}_{1}+\boldsymbol{q},\boldsymbol{k}_{2}-\boldsymbol{q})$$
(5)

where the trial wavefunction is taken as a linear combination of the product of the two electron-hole pairs formed in the system:

$$\phi_{tr}(\mathbf{k}_1, \mathbf{k}_2) = A(\phi_{\alpha,\beta}(\mathbf{k}_1)\phi_{\gamma,\kappa}(\mathbf{k}_2)$$

$$(-1)^S \phi_{\alpha,\beta}(\mathbf{k}_2)\phi_{\gamma,\kappa}(\mathbf{k}_1))$$
(6)

and the factor $(-1)^S$ changes, depending on whether the system is a singlet or a triplet. The candidate of the ground state is a singlet trion. Therefore, explicitly, the trial wavefunction of the system, using the 1s exciton wavefunction states, reads:

$$\phi_{tr}^{1s}(\mathbf{k}_{1}, \mathbf{k}_{2}) = \left(\frac{1}{(\alpha^{2} + k_{1x}^{2} + k_{1y}^{2}/\beta^{2})^{3/2}} \times \frac{1}{(\gamma^{2} + k_{2x}^{2} + k_{2y}^{2}/\kappa^{2})^{3/2}}\right) + \left(\frac{1}{(\alpha^{2} + k_{2x}^{2} + k_{2y}^{2}/\beta^{2})^{3/2}} \times \frac{1}{(\gamma^{2} + k_{1x}^{2} + k_{1y}^{2}/\kappa^{2})^{3/2}}\right)$$

$$(7)$$

Here, we assume that there is no effect of overlap of the electronic bound states, which is a valid approximation

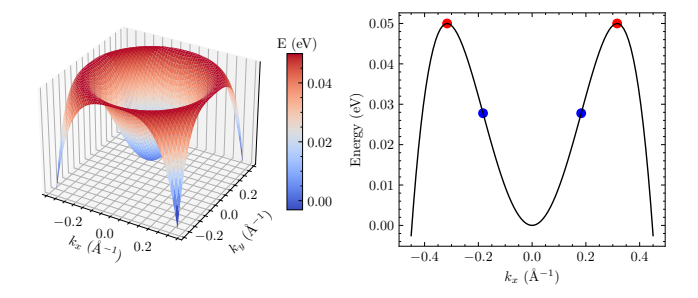


FIG. 1. Example of (inverted) Mexican-hat dispersion of form $A\mathbf{k}^2 - B\mathbf{k}^4$. (Left) Surface plot, (right) plot along k_x , where the VHS points are indicated in red and the divergent effective mass is indicated in blue.

when the band gap is much greater than the binding energy of the system.

Mexican-hat dispersions (which have a divergent effective mass) are seen in many areas of condensed matter, and their formulation can be of a simple polynomial of the form $A\mathbf{k}^2 - B\mathbf{k}^4$, or a more complicated polynomial expression up to at least 8th order, as seen for monolayer InSe [9, 29]. However, in each case the resulting band shape has the same characteristic as that shown in Fig. 1, which features a band inversion around its centre and a VHS at the band extrema and a point between the extrema at $\mathbf{k} = 0$, where the effective mass diverges.

III. MEXICAN-HAT VALENCE BAND

In this section, we investigate how the width and depth separately influence the bound states, which can form with a Mexican-hat valence band given by

$$E_v(\mathbf{k}) = A\mathbf{k}^2 - B\mathbf{k}^4. \tag{8}$$

We shall measure the width of the Mexican-hat by the value of k at the band maximum so that $k_{max} = \sqrt{A/(2B)}$ and the Mexican-hat depth by $\Delta M = E_v(k_{max}) - E_v(0) = A^2/4B$. Note that to consider the effects of purely the valence band , we assume that the effective mass of the electron in the conduction band is fixed. However, the effective mass of the conduction band also plays a role in determining the binding energies. The larger the effective mass, the shallower the band dispersion, which leads to a larger binding energy, see Appendix. B for the calculation details.

We first consider a range of different valence bands with different k_{max} but with the same $\Delta M = 0.021$ eV. To illustrate this we show in Fig. 2a, three different examples of valence bands with different k_{max} , given by the following equations

$$E_{v_1}(\mathbf{k}) = 2.33\mathbf{k}^2 - 65\mathbf{k}^4$$

$$E_{v_2}(\mathbf{k}) = 5\mathbf{k}^2 - 300\mathbf{k}^4$$

$$E_{v_3}(\mathbf{k}) = 8.16\mathbf{k}^2 - 800\mathbf{k}^4$$
(9)

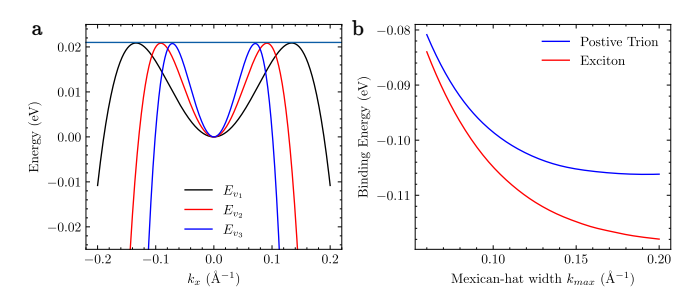


FIG. 2. (a) Valence band dispersion of the inverted Mexicanhat shaped dispersion described in Eq.(9). (b) Plot of changing Mexican-hat width k_{max} for a fixed ΔM of 0.021 eV.

so that the Mexican-hat width in each system is respectively:

$$k_{max}^1 = 0.134 \text{Å}^{-1}, \quad k_{max}^2 = 0.091 \text{Å}^{-1}, \quad k_{max}^3 = 0.071 \text{Å}^{-1}$$
(10)

The red curve in Fig.2a shows the binding energy of the exciton with increasing k_{max} . As k_{max} increases (for an equal conduction band effective mass m=0.15 in units of the bare effective mass), the excitonic state has a larger amplitude binding energy. Eventually the binding energy reaches a maximum value and limits the ground-state momentum-dark exciton energy. This is expected because, by increasing the width, the valence band gets flattened in region of k close to the conduction band minimum.

We also investigate how the positive trion of a singlet state (with spin-degenerate valence bands) varies with k_{max} , with the same set of valence bands as for the exciton. The trion binding energy follows the same behaviour as the exciton in that its binding energy amplitude increases with increasing k_{max} (blue curve in Fig. 2b). However, there is a difference when we consider purely the trion binding energy (given by the difference between three-particle and two-particle binding energies). This is that as the width decreases, the trion binding energy leads to a more favourable trion state in comparison to the exciton, despite the smaller overall binding energy. This can be seen in Fig. 2b as the decreasing difference between the excitonic and trionic binding energies.

We also investigate the effect of the Mexican-hat depth, ΔM on the exciton and trion formation. We keep the width of the Mexican-hat $k_{max} = \sqrt{A/(2B)}$ constant by fixing the ratio of A/B = C = 0.035 (so that $k_{max} = 0.132 \text{Å}^{-1}$). Then we vary A to obtain the three example dispersions shown in Fig. 3a

$$E_{v_4}(\mathbf{k}) = 1\mathbf{k}^2 - (1/C)\mathbf{k}^4$$

$$E_{v_5}(\mathbf{k}) = 5\mathbf{k}^2 - (5/C)\mathbf{k}^4$$

$$E_{v_6}(\mathbf{k}) = 10\mathbf{k}^2 - (10/C)\mathbf{k}^4$$
(11)

with Mexican hat depths respectively:

$$\Delta M_4 = 0.006 \text{ eV}, \ \Delta M_5 = 0.031 \text{ eV}, \ \Delta M_6 = 0.063 \text{ eV}$$
(12)

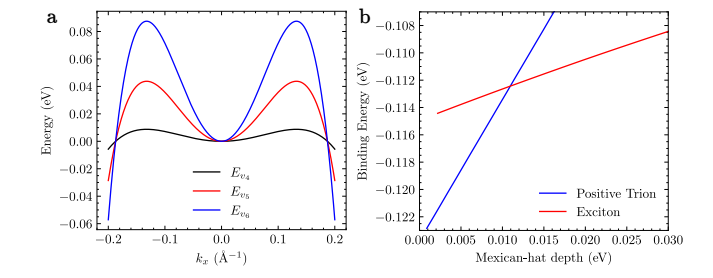


FIG. 3. (a) Valence band dispersion of the Mexican-hat forms in Eq.(11). (b) Continuous binding energies line of the exciton and trion (total) binding energies of the system, where the ratio A/B is equal to 0.035 throughout.

In Fig. 3b we show the interplay between the trion and exciton binding energies with ΔM varying from 0 to 0.03 eV. We find for smaller ΔM , the amplitude of the exciton and trion (total) binding energies increase. This general trend is expected because a smaller ΔM suggests the valence band becomes closer to the flat band regime, where we would expect the largest binding energies from consideration of the simple effective mass model. However, the trion's binding energy depends more strongly on ΔM so that it becomes more bound than the exict at small ΔM . Our analysis shows that a positive trion with a large binding energy is preferred over the formation of an exciton and a free hole, in systems with a Mexican-hat dispersion that has a narrow width and a reduced depth. For wider Mexican-hats, the bound quasiparticle which forms in the would more likely be of an excitonic type.

IV. HIGHER-ORDER VAN HOVE SINGULARITIES (HOVHS)

In this section, we investigate the effect of a different form of VHS on the formation of bound states. We will investigate this in two parts. Firstly, we add a Higher-order van-Hove singularity (HOVHS) to the existing Mexican-hat system and determine how the DOS and the bound state properties change as a result. Secondly, we investigate the case of a system that only exhibits a HOVHS in the electronic band structure. Here, the dispersion of the conduction band is taken to be parabolic with an effective mass of m=0.15.

The HOVHS we consider is the monkey-saddle (MS) which arises due to a dispersion relation of the form:

$$A\mathbf{k}^3 \cos 3\varphi = A(k_x^3 - 3k_x k_y^2) \tag{13}$$

with A>0. The DOS in this case is power-law divergent in energy $g(E)\approx A^{-2/3}|E|^{-1/3}$, the signature of a HOVHS.

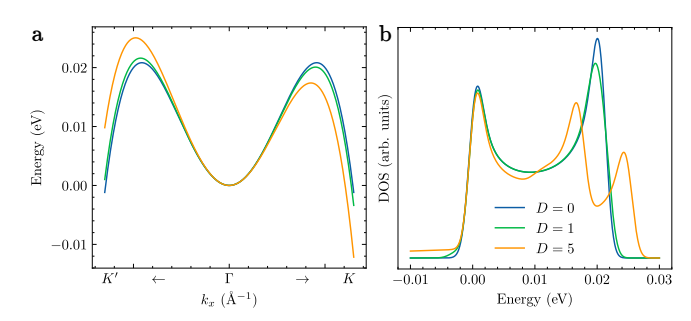


FIG. 4. Valence band dispersion (a) and DOS (b) of the Mexican-hat dispersion with monkey saddle term added, see Eq.(15). The units of D are eVÅ³.

A. Mexican-hat dispersion with a HOVHS

We now consider the following valence band dispersion corresponding to the Mexican hat dispersion with a HOVHS:

$$E_v(\mathbf{k}) = A\mathbf{k}^2 - B\mathbf{k}^4 - D\mathbf{k}^3 \cos 3\varphi \tag{14}$$

This is similar to the inclusion of the six-fold symmetry term in the valence band of monolayer InSe.

Specifically, for a fixed Mexican-hat A, B we vary D and examine how the exciton and positive trion bound states are affected through their energy dispersion and DOS calculation. We shall use $E_{v_2}(\mathbf{k})$ defined in Eq.(9):

$$E_v(\mathbf{k}) = 5\mathbf{k}^2 - 300\mathbf{k}^4 - D\mathbf{k}^3 \cos 3\varphi \tag{15}$$

To begin, we describe the energy dispersion seen for D =0 (no effect of the HOVHS term), then subsequently for $D = 1 \text{ eVÅ}^3$ and $D = 5 \text{ eVÅ}^3$. The valence bands with these values are shown in Fig. 4a, and the corresponding electronic DOS are shown in Fig. 4b. The introduction of the monkey saddle term reduces the symmetry of the system to C_3 , which in turn lifts the degeneracy of the K high symmetry points in the Brillouin zone. When D=0, each $\Gamma-K$ is symmetrically equivalent, but when $D \neq 0$ we introduce another high-symmetry point, which we denote by K'. Therefore, the valence band dispersion along $\Gamma - K$ and $\Gamma - K'$ is different, see Fig. 4a. Our calculations show the corresponding exciton dispersion also becomes inequivalent along $\Gamma - K$ and $\Gamma - K'$, see Fig. 5a. At D=0 we obtain a symmetrically equivalent Mexican-hat, but this changes with the minimum point of the dispersion being along $\Gamma - K$ whilst along $\Gamma - K'$ the Mexican-hat energy here is seen but with a lower hat depth. In addition, one can see that by including the new term, the ground-state exciton binding energy is also reduced.

The DOS is also affected by the HOVHS shown in Fig. 5b. If D=0, where the excitonic minimum is symmetrically equivalent, we obtain two peaks in the DOS: one that contributes to the momentum-dark state (lower energy) and one that contributes to the bright state (higher

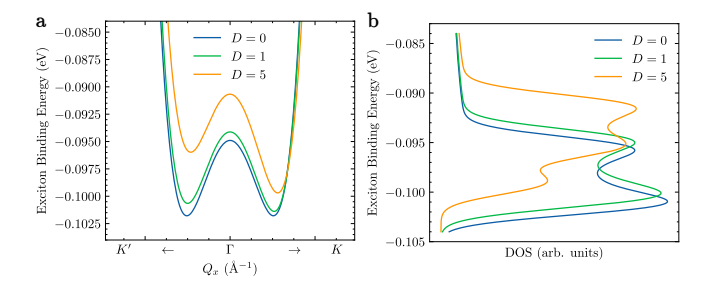


FIG. 5. (a) Excitonic dispersion of Mexican-Hat valence band dispersion with monkey saddle term added. From the system described in Fig. 4 and Eq.(15). (b) Density of states of the excitonic dispersion. The units of D are $\mathrm{eV}\mathring{\mathrm{A}}^3$.

energy). However, when $D = 5 \text{ eV}\text{Å}^3$, when the degeneracy between K and K' lines is lifted, we have an extra contribution. This is because the lowest energy state can be distinguished in energy, resulting in an additional reduced amplitude DOS peak (given it is only seen along the $\Gamma - K$ line, whilst the minimum energy along the $\Gamma - K'$ is also seen along $\Gamma - K$). This means that in this state, the momentum-dark state, although being in the ground state, may not play as important a role in the excitonic optical properties. In contrast the energy states of the minimum along the $\Gamma - K'$ line and the bright excitonic state may play a more significant role. However, the splitting of the peak may still be large enough to contribute to an extra photoluminescence peak. Although given the small change in energy for small values of D, these peaks may be hard to distinguish experimentally. The effect can be enhanced with large enough D, which causes these two states to be further apart in energy. One can further note that the amplitude of the DOS peak corresponding to the bright peak is relatively unaffected by D. However, the relative amplitude of the bright peak to dark peak is strong affected by D such that the bright state becomes relatively stronger with increasing D, where one can see for $D = 5 \text{ eV} \text{Å}^3$ how the bright state peak at Q = 0 is the largest DOS peak, whilst for D=0 and D=1 eVÅ³ it is the momentum-dark state.

B. HOVHS in the valence band

Next, we study the excitonic states that result in a valence band dispersion which is purely a monkey-saddle:

$$E_v(\mathbf{k}) = D\mathbf{k}^3 \cos 3\varphi \tag{16}$$

In this case, we consider the excitonic state which forms at the Γ -point Q=0. After following the minimisation process, we obtain, when $D=2.5~{\rm eV\AA^3}$, the exciton dispersion shown in Fig. 6. We find that the exciton dispersion has the same monkey saddle form as that of the valence band retaining its same symmetry properties.

Varying D, we find that the binding energy at the Γ point, for $D = 0.5, 1, 2.5 \text{ eV} \text{Å}^3$ is constant. However, the

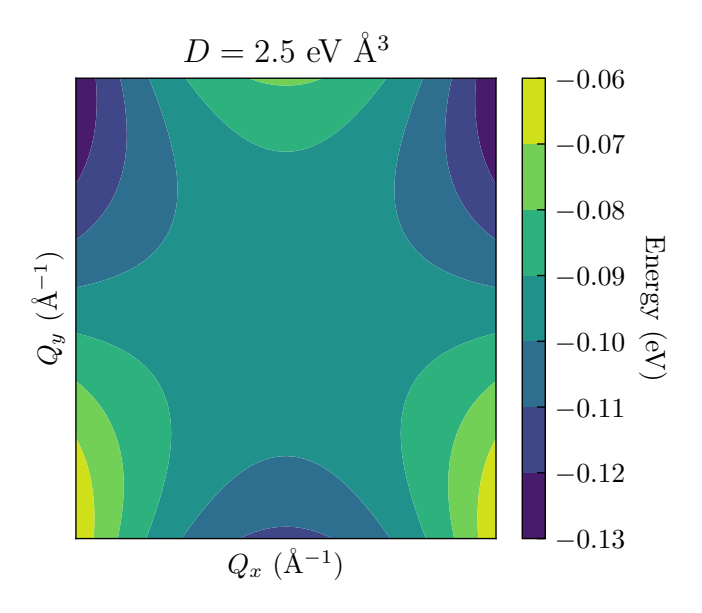


FIG. 6. Contour Plot of the excitonic dispersion in the case of the valence band being a monkey-saddle as in Eq.(16) with D=2.5 eV Å³.

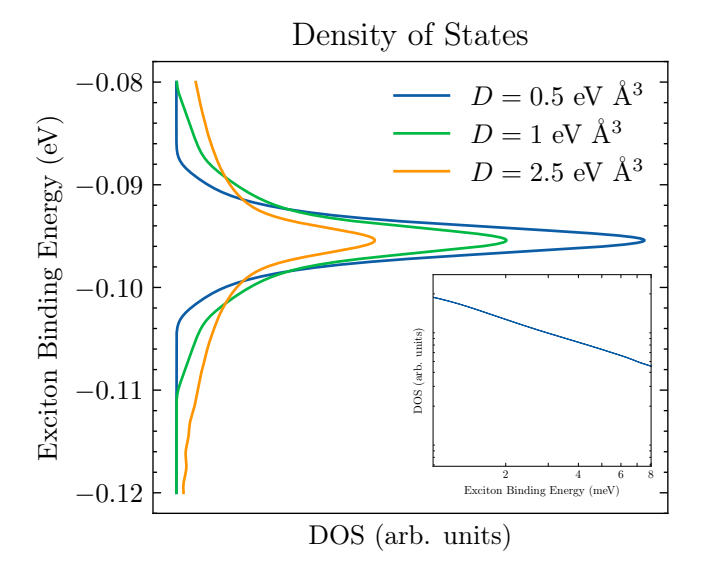


FIG. 7. DOS of Excitonic dispersion resulting from the valence band term in Eq.(16) and the contour plot in Fig. 6. (Inset) log-log plot of the exciton DOS with a MS valence band, for $D=2.5 \text{eV} \text{Å}^3$, which shows a linear relation as expected for a power-law divergence of the DOS.

DOS of the exciton is more strongly affected by D, as shown in Fig. 7.

We find that the valence band's DOS directly influences that of the excitonic DOS. In particular, we find that the exciton dispersion hosts a HOVHS. In the inset of Fig. reffig:msDOSex , we show a log-log plot of the exciton DOS dependence on energy. We find linear dependence as we approach the singularity which associated with a power law dependence of the DOS, indicating

a HOVHS [20]. Thus, a HOVHS in the valence band is also reflected in the bound state exciton.

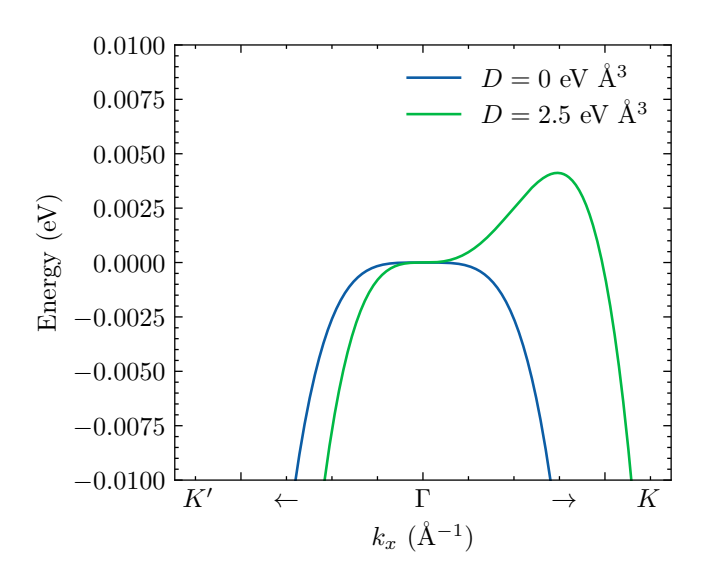


FIG. 8. Valence band dispersion for changing value of D from Eq.(14), transferring from a direct to indirect semiconductor system as D goes from zero to non-zero.

This suggests the possibility of engineering a VHS or HOVHS that exhibits a large peak in the momentum dark excitonic DOS, which is substantially larger than that of the bright state. If the momentum-dark bound state contribution to the optical properties of a material dominates then the lifetime of these bound ground states could be extended significantly.

To demonstrate this, we take a bright excitonic system in which the conduction band has the usual parabolic form given by

$$E_c(k) = A\mathbf{k}^2 \tag{17}$$

and the valence band has the following k^4 dependence

$$E_v(\mathbf{k} - \mathbf{Q}) = -B(\mathbf{k} - \mathbf{Q})^4. \tag{18}$$

We add the HOVHS term to the valence band as a perturbation so that it becomes:

$$E_v(\mathbf{k} - \mathbf{Q}) = -B(\mathbf{k} - \mathbf{Q})^4 \pm D(\mathbf{k} - \mathbf{Q})^3 \cos 3\varphi \quad (19)$$

which shifts the VBM away from the Γ point to some finite position along $\Gamma - K$. We consider values of D = 0 and D = 2.5 eVÅ³ and $A = 1/2m_e$ where $m_e = 0.15$ and B = 10 eVÅ⁴. We obtain the valence bands shown in Fig. 8. We see that by including a non-zero value of D, we obtain a one-sided Mexican-hat with a width and depth that increases with D. The calculation of the exciton dispersion reveals that although width increases (which would itself lead to a larger binding energy), the increase in depth dominates the properties of the bound state subsequently decreasing the binding energy. Whilst both of these effects compete with one another, the depth

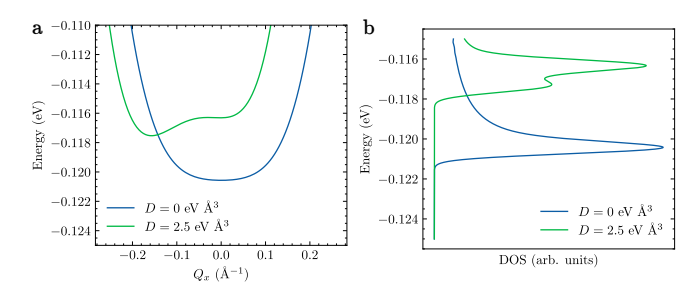


FIG. 9. (a) Excitonic dispersion for the changing valence band structure in Fig. 8. (b) Density of states of the excitonic dispersion.

is a more important factor in determining how bound the exciton is; thus, one would expect the amplitude of the binding energy for increasing D to decrease. This is shown in Fig. 9. Therefore, it can be concluded that the introduction of the C_3 -symmetry perturbation in the form of the monkey-saddle HOVHS leads to a decrease in the overall DOS. However, this suggests that a system can be engineered from an initial bright excitonic system to one where we have not only a bright state but also a momentum-dark peak that influences the subsequent optical properties of the system. This may enhance the lifetime of the bound states which can form in a particular system.

V. DISCUSSION AND CONCLUSIONS

In this work, first we investigated exciton and trion formation in Mexican-hat shaped systems, then we analysed the effect of a including a HOVHS in the valence band. Our work shows that as the width of the Mexican-hat is increased (defined as the distance between $\mathbf{k}=0$ and the brim of the hat), the overall binding energy of the excitons and trions increases. In addition, as the depth of the Mexican hat is increased, the overall binding energy of the two and three-particle systems decreases. For the trion binding energy (defined as the difference between three particle and two particle overall binding energies), a trion to be more favourable for a given depth, one requires a narrower Mexican-hat.

Our work on HOVHS suggests that valence bands with this type of singularity could lead to bound-state quasiparticles with the same type of singularity in their DOS allowing us to enhance the optical properties. In principle, the example of a HOVHS of a monkey-saddle type is developed at the K-points of the Brillouin zone in Bernal stacked bilayer graphene in the system [30]. Therefore, we expect our results for the excitonic state at the HOVHS will be directly relevant to this work. However, we expect that, for the case of a trion, spin orbit coupling will play a more important role.

Our results indicate that it is possible to generate new states at a different energy, that will affect the optical properties of the system. This applies both to systems with an initially bright excitonic ground state and to momentum-dark configurations, such as those arising from Mexican-hat-shaped valence band dispersions. In momentum-dark states, the lifetime is extended because an additional scattering process is required for the electron-hole pair to reach a radiative recombination state. This longer lifetime makes these states controllable, a key requirement for designing novel quantum devices [31–33].

Finally, we provide new insights into how VHSs influence the formation of exciton and trion bound states. For a standard (logarithmic in 2D) VHS associated with a Mexican-hat dispersion, we demonstrated that the resulting bound states are highly sensitive to changes in the electronic band structure. Furthermore, the inclusion of a HOVHS can play an important role in tuning and

enhancing the optical properties of the material under question, such as the formation of momentum-dark excitons and trions. If such effects could be experimentally controlled, they could significantly expand the potential of these 2D materials for a wide range of optoelectronic applications.

ACKNOWLEDGMENTS

We would like to thank David Perkins and Ioannis Rousochatzakis for useful discussions. The work has been supported by the EPSRC grants $\rm EP/T034351/1$ and $\rm EP/X012557/1$.

- [1] J. Frenkel, Physical Review **37**, 17 (1931).
- [2] M. A. Lampert, Physical Review Letters 1, 450 (1958).
- [3] C. Zhang, H. Wang, W. Chan, C. Manolatou, and F. Rana, Phys. Rev. B 89, 205436 (2014).
- [4] H. Wang, C. Zhang, W. Chan, C. Manolatou, S. Tiwari, and F. Rana, Phys. Rev. B 93, 045407 (2016).
- [5] D. Vaclavkova, J. Wyzula, K. Nogajewski, M. Bartos, A. O. Slobodeniuk, C. Faugeras, M. Potemski, and M. R. Molas, Nanotechnology 29, 325705 (2018).
- [6] R. Tempelaar and T. C. Berkelbach, Nature Communications 10, 10.1038/s41467-019-11497-y (2019).
- [7] F. Rana, O. Koksal, and C. Manolatou, Phys. Rev. B 102, 085304 (2020).
- [8] S. Shradha, R. Rosati, H. Lamsaadi, J. Picker, I. Paradisanos, M. T. Hossain, L. Krelle, L. Oswald, N. Engel, D. Markina, et al., arXiv preprint arXiv:2510.21422 (2025).
- [9] A. Ceferino, K. W. Song, S. J. Magorrian, V. Zólyomi, and V. I. Fal'ko, Phys. Rev. B 101, 245432 (2020).
- [10] L. J. Burke, M. T. Greenaway, and J. J. Betouras, npj 2D Materials and Applications 9, 63 (2025).
- [11] M. Brotons-Gisbert, H. Baek, A. Campbell, K. Watanabe, T. Taniguchi, and B. D. Gerardot, Physical Review X 11, 031033 (2021).
- [12] M. Brotons-Gisbert, B. D. Gerardot, A. W. Holleitner, and U. Wurstbauer, MRS bulletin 49, 914 (2024).
- [13] C. Lui, A. Frenzel, D. Pilon, Y.-H. Lee, X. Ling, G. Akselrod, J. Kong, and N. Gedik, Physical review letters 113, 166801 (2014).
- [14] E. Liu, J. van Baren, Z. Lu, M. M. Altaiary, T. Taniguchi, K. Watanabe, D. Smirnov, and C. H. Lui, Phys. Rev. Lett. 123, 027401 (2019).
- [15] M. R. Molas, C. Faugeras, A. O. Slobodeniuk, K. No-gajewski, M. Bartos, D. Basko, and M. Potemski, 2D Materials 4, 021003 (2017).
- [16] E. Malic, M. Selig, M. Feierabend, S. Brem, D. Christiansen, F. Wendler, A. Knorr, and G. Berghäuser, Physical Review Materials 2, 014002 (2018).
- [17] M. Zinkiewicz, A. Slobodeniuk, T. Kazimierczuk, P. Kapuściński, K. Oreszczuk, M. Grzeszczyk, M. Bartos, K. Nogajewski, K. Watanabe, T. Taniguchi, et al., Nanoscale 12, 18153 (2020).

- [18] R. Perea-Causin, S. Brem, O. Schmidt, and E. Malic, Physical Review Letters 132, 036903 (2024).
- [19] L. Van Hove, Phys. Rev. 89, 1189 (1953).
- [20] A. Chandrasekaran and J. J. Betouras, Phys. Rev. B 105, 075144 (2022).
- [21] L. Classen and J. J. Betouras, Annual Review of Condensed Matter 16, 229 (2025).
- [22] A. Chandrasekaran, L. C. Rhodes, E. A. Morales, C. A. Marques, P. D. C. King, P. Wahl, and J. J. Betouras, Nature Communications 15, 9521 (2024).
- [23] A. Chandrasekaran and J. J. Betouras, Advanced Physics Research 2, 2200061 (2023).
- [24] V. Zólyomi, N. Drummond, and V. Fal'Ko, Physical Review B 89, 205416 (2014).
- [25] N. S. Rytova, arXiv preprint arXiv:1806.00976 (2018).
- [26] L. V. Keldysh, Soviet Journal of Experimental and Theoretical Physics Letters 29, 658 (1979).
- [27] H. J. Monkhorst and J. D. Pack, Phys. Rev. B 13, 5188 (1976).
- [28] J. D. Pack and H. J. Monkhorst, Phys. Rev. B 16, 1748 (1977).
- [29] S. J. Magorrian, V. Zólyomi, and V. I. Fal'ko, Physical Review B 94, 245431 (2016).
- [30] A. Shtyk, G. Goldstein, and C. Chamon, Phys. Rev. B 95, 035137 (2017).
- [31] T. Chowdhury, S. Chatterjee, D. Das, I. Timokhin, P. D. Núñez, G. M. A, S. Chatterjee, K. Majumdar, P. Ghosh, A. Mishchenko, et al., Physical Review B 110, L081405 (2024).
- [32] H. Qu and Y. Li, Physical Review B 107, 235407 (2023).
- [33] N. T. Paylaga, C.-T. Chou, C.-C. Lin, T. Taniguchi, K. Watanabe, R. Sankar, Y.-h. Chan, S.-Y. Chen, and W.-H. Wang, npj 2D Materials and Applications 8, 12 (2024).

Appendix A: Dependence on the dielectric environment

Here we investigate the effect of the product of the in-plane $\kappa_{||}$ and out-of-plane κ_{z} permittivities, seen in Eq.(2), on the binding energy for a fixed valence band and conduction band, see Fig. 10. We find that as the product of the out-of-plane and in-plane permittivity decreases, the binding energy of the exciton increases. In other words, the binding energy is increased with increased screening length.

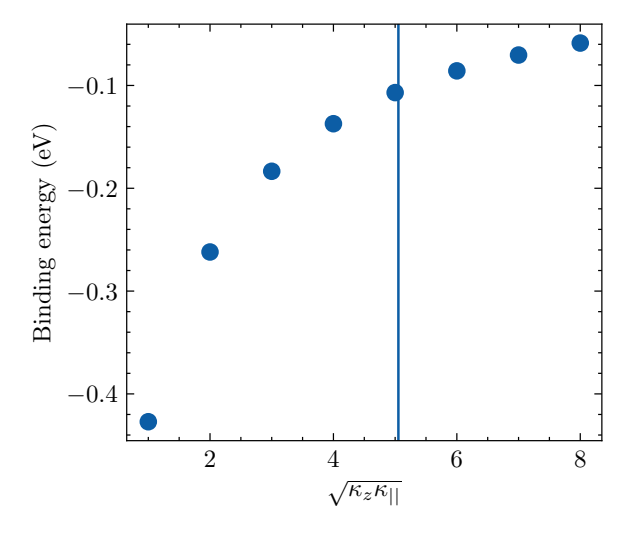


FIG. 10. Plot of $\sqrt{\kappa_z \kappa_{||}}$ against exciton binding energy, vertical line indicates the encapsulation of hBN as used in this work. This changes the strength of the Coulomb interaction via the Rytova-Keldysh potential as shown in Eq.(2).

Appendix B: Dependence on electron effective mass

Here, we consider the effects that the conduction band has on a fixed Mexican-hat shaped dispersion. We therefore consider different effective masses in the expression energy dispersion $E_c(\mathbf{k}) = \frac{1}{2m_e^*}\mathbf{k}^2$. We take the values: $m_e^* = 0.05, 0.15, 0.25, 0.35$, in units of the bare electron mass m_e . We also introduce a simplified Mexican-hat energy dispersion of the form: $E_v(\mathbf{k}) = A\mathbf{k}^2 - B\mathbf{k}^4$, where the units of A and B are eVÅ 2 and eVÅ 4 respectively. The inset of Fig. 11 illustrates the change in the shape of the conduction band with these different effective masses. In Fig. 11, we show the results of our calculation of the excitonic dispersion with different effective masses. We use the minimisation process with respect to the 1s ground state, Eq.(4). We find that an increased effective mass results in an increased binding energy of the exciton.

In addition, the minimum energy state becomes more momentum-dark, with a momentum further away from Q = 0. This behaviour is due to the flattening of the conduction band, leading to a larger binding energy.

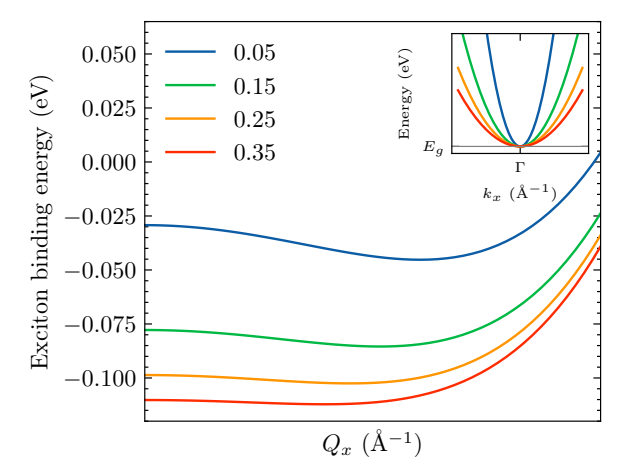


FIG. 11. Exciton energy dispersion for a fixed valence band, $E_v(\mathbf{k}) = A\mathbf{k}^2 - B\mathbf{k}^4$ for four values of the electron effective mass in the conduction band. Inset: Comparison of the parabolic conduction bands with different values of the effective mass.

Appendix C: Impact of Brillouin zone size

In the study of the width of the Mexican hat, one needs to investigate the impact of the Brillouin zone (BZ) width. In this work we choose the BZ to be defined 1.4 times further along $\Gamma - K$ past k_{max} . To show the influence of this parameter, we consider one Mexican-hat valence band $E_{v_2}(\mathbf{k})$ and modify the size of the BZ by a factor W > 1 so that

$$BZ_{width} = Wk_{max} = W\left(\frac{A}{2B}\right)^{1/2}$$
 (C1)

The effective BZ is increased in area by a factor W^2 . The results for the binding energy for W=1.2, 1.4 and 1.6 are shown in Fig. 12 which shows that the further away from the VBM of the Mexican-hat the edge of the BZ is, the larger the binding energy of the quasiparticle states becomes. However, one also finds that the trion binding energy (difference between three and two particle binding energies) doesn't scale in this way; in fact, to 3 decimal places, the trion binding energy remains 5 meV throughout. Thus, the trion binding energy does not depend on how far away from the VBM the defined grid edge is.

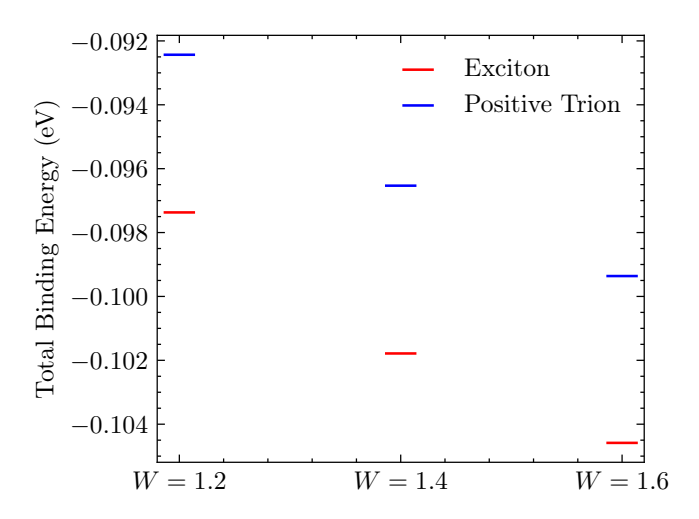


FIG. 12. Plot of Exciton and positive trion (total) binding energies against different effective BZs.